ELSEVIER

Journal of Molecular Catalysis A: Chemical 159 (2000) 335–345

JOURNAL OF MOLECULAR CATALYSIS A: CHEMICAL

www.elsevier.com/locate/molcata

Catalytic decomposition of CFC-12 over solid acids WO_3/M_xO_y (M = Ti, Sn, Fe)

Zhen Ma, Weiming Hua, Yi Tang, Zi Gao *

Department of Chemistry, Fudan University, Shanghai, 200433, People's Republic of China

Received 25 December 1999; received in revised form 25 February 2000; accepted 25 February 2000

Abstract

Catalytic decomposition of dichlorodifluoromethane (CFC-12) in the presence of water vapor was investigated over a series of pure and WO_3-promoted metal oxides. Although pure TiO_2, SnO_2 and Fe_2O_3 showed less activity for the decomposition of CFC-12, obvious enhancement in activity was actualized by supporting WO_3 on them using $Ti(OH)_4$, $Sn(OH)_4$ and $Fe(OH)_3$ as support precursors. The decomposition activity depended on the calcination temperature obviously and attained to a maximum as the content of WO_3 reached its utmost dispersion capacity on different supports. The 95% conversion temperature of WTi, WSn and WFe catalysts prepared by optimum conditions were 260°C, 315°C and 345°C, respectively. CO_2 was the main-product and no CO was detected as by-product. The selectivity to by-product CFC-13 on WO_3-modified metal oxides was much lower than on unmodified metal oxides and it also exhibited a coverage-dependent effect. The catalytic activity of WO_3/TiO_2, WO_3/SnO_2 and WO_3/Fe_2O_3 all remained steady for 120 h on stream.

Keywords: Freon decomposition; Solid acids; Tungsten oxide; Titania; Tin oxide; Iron oxide

1. Introduction

CFCs (chlorofluorocarbons) are a family of industrial compounds widely used as refrigerants, solvents, propellants, blowing agents, etc. However, in 1974, Molina and Rowland published a paper in Nature, pointing out that CFCs are killers of the ozone layer that protects life on earth against harmful ultraviolet radiation from the sun [1]. This conclusion has been continuously confirmed by thousands of studies [2]. As a result, the Montreal Protocol, an international treaty to phase out and control CFCs, was signed by 163 countries and the 1995's Nobel Prize in chemistry said yes to Molina and Rowland [3]. Further investigations also indicated that CFCs are greenhouse gases that are warming up our earth. As earth warms up, disease threats will increase and icebergs will break away [4].

In order to tackle these environmental problems, many CFCs were banned without delay; however, there are still 2.25 million-ton CFCs all over the world and numerous air-condition-

* Corresponding author. Tel.: +86-21-65642792; fax: +86-21-65641740.

E-mail address: xhdeng@fudan.edu.cn (Z. Gao).

1381-1169/00/$ - see front matter
PII: S1381-1169(00)00191-6

ing systems still use them. These CFCs are leaking out of existing equipments and will not be degraded in nature for a century because of their chemical inertness. Therefore, techniques that can eliminate CFCs either prior to or during their release to the environment are extremely desired.

The CFC decomposition has attracted considerable public enthusiasm. A dozen of decomposition approaches such as incineration, cement kiln, high frequency-induced plasma, super critical water, electrochemical decomposition, ultrasonic irradiation, reduction with sodium naphthalenide and catalytic decomposition have been developed so far. Catalytic decomposition is very promising because of simple processes, requiring mild conditions and free dioxins [5,6]. Investigations in this direction have been continuously pursued by dozens of groups for a decade and several reviews have been published [7–9]. Many catalysts, such as zeolites [10,11], pure and transition metal chloride promoted γ-Al_2O_3 [12], SiO_2–Al_2O_3 [13], V_2O_5/Al_2O_3 [14], fluorinated TiO_2 [15], TiO_2–SiO_2 [16], TiO_2–ZrO_2 [17], Pt/ZrO_2–TiO_2 [18], Cr_2O_3/ZrO_2 [19] and BPO_4 [20] were found to be active for CFC decomposition. More recently, Takita et al. [21–23] reported that metal phosphates such as $AlPO_4$ and $Zr_3(PO_4)_4$ also showed high activity in this reaction; however, there's still some room for improving the catalytic activity, selectivity and stability.

Although the CFC decomposition mechanism has not been fully illuminated, it's interesting to note that all the efficient catalysts mentioned above are solid acids, while other materials such as CaO, SiO_2, carbon, ZnO, MgO and Fe_2O_3 showed rare activity for this reaction. This information may provide a useful clue to design efficient CFC decomposition catalysts. Our group has continuously carried out the fundamental research of solid strong acids for 10 years [24–29]. The authors noticed that Hino and Arata prepared three solid strong acids WO_3/TiO_2, WO_3/SnO_2 and WO_3/Fe_2O_3 by impregnating $Ti(OH)_4$, $Sn(OH)_4$ and $Fe(OH)_3$ with ammonium metatungstate and then calcining in air [30]. These catalysts were active for the skeletal isomerization and cracking of isopentane. In this paper, the catalytic decomposition of CFC-12 over WO_3/TiO_2, WO_3/SnO_2 and WO_3/Fe_2O_3 catalysts with high activity, selectivity and stability will be reported. Furthermore, the reasons why these catalysts showed high activity, selectivity and stability will be discussed in detail.

2. Experimental

2.1. Catalyst preparation

$Ti(OH)_4$, $Sn(OH)_4$ and $Fe(OH)_3$ were obtained by hydrolyzing guaranteed grade reagents of $TiCl_4$, $SnCl_4$ and $Fe(NO_3)_3$, respectively, with ammonium hydroxide, washing, drying at 110°C and powdering. The hydroxides were impregnated with aqueous ammonium metatungstate $[(NH_4)_6(H_2W_{12}O_{40})]$ followed by evaporating water, drying at 110°C, calcining in air at different temperatures for 3 h. These catalysts were labeled as WM*n*–*m*, where *n* means the WO_3 content (g/g metal oxide) and *m* stands for the calcination temperature. For comparison, M_xO_y (M = Ti, Sn, Fe) were prepared by calcining $Ti(OH)_4$, $Sn(OH)_4$ and $Fe(OH)_3$ at corresponding temperatures.

2.2. Reaction testing

The catalytic decomposition was carried out at atmospheric pressure using a fixed-bed flow microreactor made of quartz (8 mm o.d., 6.5 mm i.d.). CFC-12 (1000 ppm), water vapor (6000 ppm) and balance air were mixed up and passed through 0.4 g catalyst with space velocity (WHSV) 6 l h^{-1} g-cat^{-1}. Reaction temperature was varied by using an electric furnace and a temperature controller. Effluent gases were passed through KOH solution to eliminate HF and HCl produced during the reaction.

Before the KOH trap, gases were collected and identified. The main product was CO_2 and no CO by-product was detected for all the catalysts. However, another by-product was detected. GC-MS confirmed that it was CFC-13. After the KOH trap, unreacted CFC-12 and by-product CFC-13 were separated with a Apiezon grease L/SiO_2 (0.7 m) column at 70°C, then analyzed by a gas chromatography equipped with a flame ionization detector (FID). The conversion of CFC-12 and selectivity to CFC-13 were calculated as follows: [Conversion of CFC-12] = ([CFC-12]in − [CFC-12]out)/[CFC-12]in × 100%; [Selectivity to CFC-13] = [CFC-13]out/([CFC-12]in − [CFC-12]out) × 100%.

2.3. Catalyst characterization

According to literature [31], NH_3–TPD of the samples was carried out in a flow-type fixed-bed reactor at ambient pressure. The adsorption temperature of NH_3 was 120°C, and the temperature was raised up at a rate of 10°C/min to desorb NH_3. The desorption spectrum was recorded by an electronic graphic drawer simultaneously and the desorbed NH_3 was accumulated in a U-type stainless steel tube immersed in a liquid N_2 trap. Then the liquid N_2 trap was replaced by a bottle of boiling water quickly to gasify all the trapped NH_3. The gasified NH_3 was quantitatively analyzed by gas chromatography. X-ray powder diffraction (XRD) measurements were performed on a Rigaku D/MAX-IIA instrument using Cu Kα radiation with 16°/min scan speed and 10–70° scan range. Laser Raman spectra (LRS) in the 200–1200 cm^{-1} range were recorded on a computer-controlled Nicolet 760 FT-Raman module. A laser power of 310 mV was used. BET surface area, pore volume and pore size distribution were measured on a Micrometritics ASAP 2000 system under liquid N_2 temperature using N_2 as absorbate. Carbon deposit was analyzed by elementary analysis.

3. Results and discussion

3.1. Effect of calcination temperature on the decomposition activity

Fig. 1 shows the CFC-12 decomposition activity over WTi, WSn and WFe series catalysts

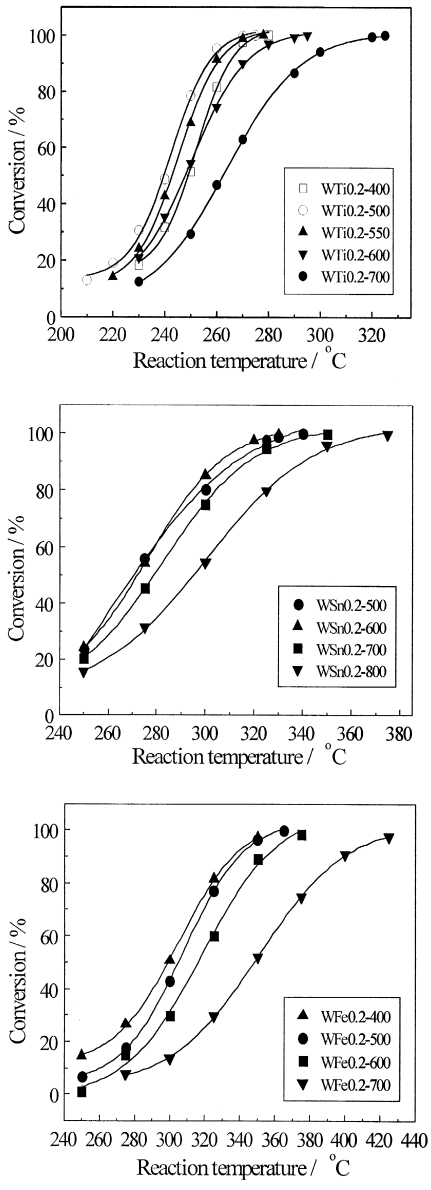

Fig. 1. Effect of calcination temperature on the CFC-12 conversion over WTi, WSn and WFe series catalysts, catalyst: 0.4 g.

calcined at different temperatures. All measurements reported here were obtained at steady state conditions. In general, steady state conditions were reached after about 40 min and 2 h of operation with WO_3/M_xO_y and M_xO_y (M = Ti, Sn, Fe). It's clear that the calcination temperature of catalysts affected the catalytic activity. The CFC-12 conversion over WTi and WSn series catalysts raised slightly and then decreased obviously with the calcination temperature, while the activity on WFe decreased monotonely as the calcination temperature was raised up. In general, high calcination temperatures are not preferred. For example, the 95% conversion temperature (T_{95}) of WTi0.2–500 was 260°C, while the T_{95} of WTi0.2–700 amounted to 305°C. Very similar tendency was reported in the ethanol synthesis [32], a typical acid-catalyzed reaction catalyzed by WO_3/TiO_2.

Okazaki [13] reported that the decomposition rate of CFC-13 on SiO_2–Al_2O_3 decreased obviously with the calcination temperature. Bickle et al. [18] once studied the CFC-113 decomposition over Pt/ZrO_2 and found that the initial activity of the 900°C-calcined catalyst was lower than others calcined at 550°C or 750°C; thus they concluded that the different calcination temperatures may affect the number of acid sites for reaction.

In this study, NH_3–TPD was used to examine if their explanation can also illuminate our results. Take WTi series catalysts for example. There was only one asymmetric broad peak on the TPD profile of all the samples and the peak temperatures ranged between 260°C and 300°C (Fig. 2), showing that most of the acid sites of the samples were of medium–strong strength. The order of the number of acid sites on samples was: WTi0.2–500 (0.740 mmol/g) > WTi0.2–550 (0.728 mmol/g) > WTi0.2–400 (0.676 mmol/g) > WTi0.2–600 (0.430 mmol/g) > WTi0.2–700 (0.413 mmol/g), which is quite in agreement with the CFC-12 decomposition activity over these catalysts, implying that the different calcination temperatures may affect the number of acid sites thus the decomposition activity.

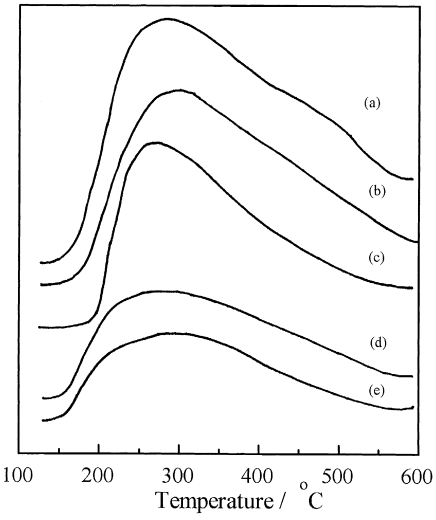

Fig. 2. NH_3–TPD profiles of WTi series catalysts calcined at different temperatures, sample: 0.2 g. (a) WTi0.2–500, (b) WTi0.2–550, (c) WTi0.2–400, (d) WTi0.2–600, (e) WTi0.2–700.

The SSA of WTi0.2–*m* series catalysts also decreased obviously with the calcination temperatures. They were 115.9, 93.0, 80.9, 54.2 and 37.6 m^2/g, respectively. It may not be concluded that SSA always determined the decomposition activity. For instance, MCM-41 molecular sieve with SSA near 1000 m^2/g was tentatively used as catalyst for this reaction, while the activity was poor because of the poor acidity of MCM-41. However, in the same catalyst system such as WTi, different calcination temperature influences the structure and properties of catalysts simultaneously. There may be some interrelationship between the SSA and amount of acid sites, thus SSA and amount of acid sites showed almost the same tendency with the catalytic activity.

3.2. Effect of WO_3 loading on the decomposition activity

Fig. 3 compares the CFC-12 conversion on pure and WO_3-loaded metal oxides. It's clear that pure TiO_2, SnO_2 and Fe_2O_3 showed poor activity. They decomposed CFC-12 completely

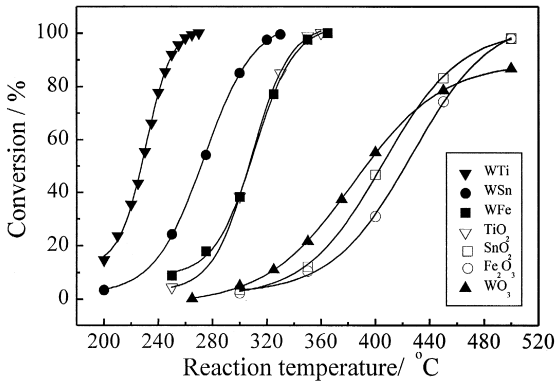

Fig. 3. CFC-12 conversion on pure and WO_3-loaded metal oxides, catalyst: 0.4 g.

at 360°C, 500°C and 500°C, respectively. WO_3 itself was also inactive, too. Its activity was only 84% even at 500°C. However, when WO_3 was supported on TiO_2, SnO_2 and Fe_2O_3, a drastic enhancement in activity was found. The T_{95} of WTi0.4–500, WSn0.2–600 and WFe0.3–500 were 255°C, 315°C and 345°C, respectively.

As recognized by many researchers, acid center is very important for the decomposition of CFCs [12–23]. Even in the HFC dehydrofluorination and CFC disproportionation reactions, acid center is also decisive [33,34]. Though both parent metal oxides showed poor activity for the decomposition of CFC-12, a generation of acid sites by a combination of two oxides is very clear, which is well illuminated by Tanabe's hypothesis [35]. The model structure of WO_3/TiO_2 was presented, and they concluded that the excess positive charge of WO_3/TiO_2 system caused the generation of Lewis acidity. If a small amount of water molecule exists on the surface, the Lewis acid sites would convert into Bronsted acid sites [36]. In fact, active CFC decomposition catalysts such as TiO_2–SiO_2, SiO_2–Al_2O_3, ZrO_2–TiO_2, V_2O_5/Al_2O_5 and Cr_2O_3/ZrO_2 were also designed by the combination of two oxides.

Fig. 4 shows the NH_3–TPD profiles of the neat and typical WO_3-promoted metal oxides. The amount of acid sites of samples followed the order: WTi0.4–500 (0.784 mmol/g) > WSn0.2–600 (0.525 mmol/g) > WFe0.3–500 (0.481 mmol/g) > TiO_2 (0.309 mmol/g) > SnO_2 (0.290 mmol/g) > Fe_2O_3 (0.264 mmol/g) > WO_3 (0.157 mmol/g). This is in agreement with the activity order of these catalysts. It should be noted that TiO_2 possessed less acid sites than WFe0.3–500, while the activities of both catalysts were similar to each other. This is because of surface fluorination of TiO_2 during the initial hours on stream [15]. The consequence of surface fluorination was the enhancement in acidity, and thus activity, of TiO_2 during the reaction. As discussed later in this paper, amorphous tungsten oxide highly dispersed on the surface of Fe_2O_3, thus suppressed the surface fluorination of WFe catalyst. This is the reason why steady state conditions were reached after about 40 min on stream for WO_3/M_xO_y; however, it took 2 h of operation for M_xO_y (M = Ti, Sn, Fe).

Furthermore, our experiments also indicated that the different WO_3 loading affected the activity, too. As shown in Fig. 5, the activity went on with the WO_3 loading until the loading exceeded a certain value, then the conversion

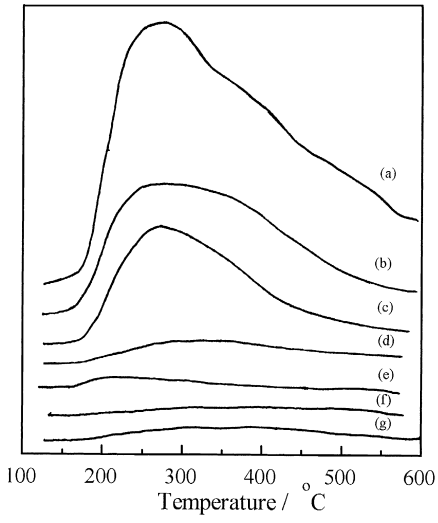

Fig. 4. NH_3–TPD profiles of pure and WO_3-loaded metal oxides, sample: 0.2 g. (a) WTi0.4–500, (b) WSn0.2–500, (c) WFe0.3–500, (d) TiO_2, (e) SnO_2, (f) Fe_2O_3, (g) WO_3.

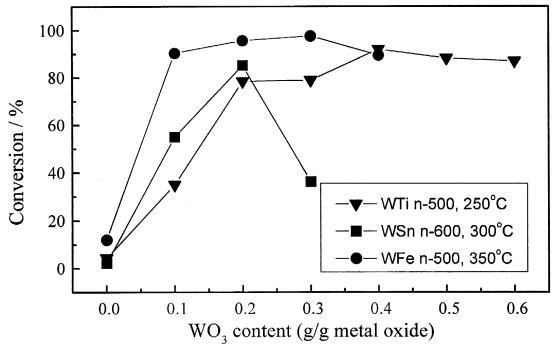

Fig. 5. CFC-12 conversion on WTi, WSn and WFe series catalysts with different WO_3 loading, catalyst: 0.4 g.

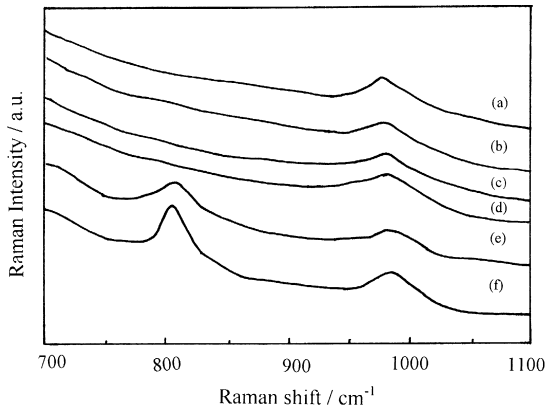

Fig. 7. LRS patterns of WTi catalysts with different loading: (a) WTi0.1–500, (b) WTi0.2–500, (c) WTi0.3–500, (d) WTi0.4–500, (e) WTi0.5–500, (f) WTi0.6–500.

dropped. The ''certain value'' for WTi, WSn and WFe series catalysts was 0.4 g/g TiO_2, 0.2 g/g SnO_2 and 0.3 g/g Fe_2O_3, respectively.

Fig. 6 compares the XRD patterns of WTi, WSn and WFe catalysts whose WO_3 content were around the value. It can be seen from the figure that no crystalline WO_3 peaks was found when the content of WO_3 = the ''certain value''; however, when W/M > the ''certain value'', characteristic peaks of crystalline WO_3 were detected. LRS is a very powerful technique in detecting the presence of the different crystalline and amorphous oxide phases on the surface of metal oxides. Now, the case study focused on the LRS of WTi catalysts (Fig. 7). The Raman peak at $\sim 980\ cm^{-1}$, which is associated with the symmetrical W=O stretching mode of the highly dispersed amorphous tungsten oxide species [37,38], was detected for all the WTi catalysts. In addition, when WO_3 content = 0.4 g/gTiO_2, no Raman peak that appeared at $\sim 800\ cm^{-1}$ was detected, indicating the absence of crystalline WO_3. But when WO_3 content is > 0.4 g/g TiO_2, the peak at $\sim 800\ cm^{-1}$ assigned to the W–O stretching model of crystalline WO_3 was detected and increased with further loading, which is consistent with the XRD results. It can then be concluded that the ''certain value'' corresponded to the utmost dispersion capacity of WO_3 on different supports.

NH_3–TPD of several typical samples was measured. The amount of acid sites followed the order: WTi0.4–500 (0.784 mmol/g) > WTi0.6–500 (0.749 mmol/g) > WTi0.2–500 (0.740 mmol/g) > WTi0.1–500 (0.493 mmol/g) > WTi0–500 (0.309 mmol/g), which is also in good agreement with the order of their activities.

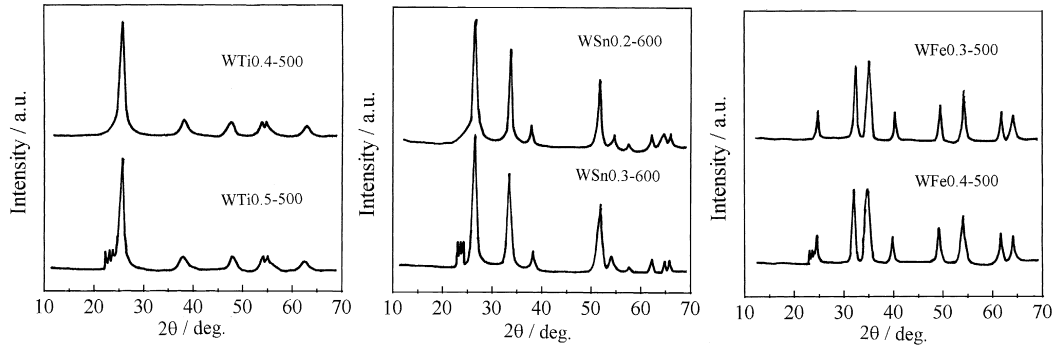

Fig. 6. XRD patterns of typical WTi, WSn and WFe samples below and above the utmost dispersion capacity of WO_3.

Table 1
Effect of WO_3 content on the selectivity to CFC-13, catalyst: 0.4 g

Catalyst	Selectivity to CFC-13 (%)						
	WO_3 content (g/g TiO_2)						
	0	0.1	0.2	0.3	0.4	0.5	0.6
WTi*n*–500	4.88	1.01	0.29	0.25	0.18	0.14	0.11
WSn*n*–600	3.58	0.58	0.43	0.42	–	–	–
WFe*n*–500	4.81	0.58	0.45	0.40	0.33	–	–

In general, an acidic oxide dispersed on the surface of a support often causes the acidity of the surface to increase and attains the highest value as the content of the oxide reaches the dispersion capacity [39]. Below the dispersion capacity, acidic oxide is dispersed as monolayer, so that the amount of surface acid sites increases with acidic oxide content. When the content of active component exceeds its dispersion capacity, excess acid oxides accumulate to form small crystals and block the pores of support, thus covering the active centers. Apart from evidences given by XRD, LRS and NH_3–TPD, another evidence was provided by BET: SSA of WTi0.4–500 was 119.4 m^2/g, while the SSA of WTi0.5–500 and WTi0.6–500 decreased to 102.8 and 99.9 m^2/g, respectively. This also confirmed that when the content of WO_3 exceeded its dispersion capacity, excess acidic oxide accumulated to form small crystal and blocked the pores of support, thus covered the active centers [40]. In addition, the SSA of WTi amounted to about 120 m^2/g and the dispersion threshold of WO_3 on the TiO_2 surface was 0.40 g/g TiO_2. Considering the SSA and mass composition of WTi, the calculated threshold was 0.24 g WO_3/(100 m^2 TiO_2). By a close-packed monolayer model, supposing WO_3 is dispersed on the surface of TiO_2 carrier, the capacity of WO_3 on 100 m^2 carrier surface is 0.21 g [41]. Our experimental result agrees with the calculated value approximately. This spontaneous dispersion phenomenon is very widespread in catalysis and can provide a useful way to design efficient catalysts [41].

3.3. Selectivity to CFC-13

CFC-13 and CO might be detected as by-products in the CFC decomposition reaction. Since they are both environmental pollutants, their formation is not preferred at all. In our results, CO_2 was the main-product and no CO was found over all the catalysts. The selectivity to CFC-13 on WO_3-modified metal oxides was much less than that on pure metal oxides (Tables 1 and 2).

Ng et al. [12] suggested that the active centers for CFC-12 fluorination are not present on the pure alumina but are formed by the fluorination of γ-Al_2O_3. Fu et al. [42] pointed out that CFC-13 was formed only when the TiO_2 surface was fluorinated, while the fluorination of TiO_2 stands for partial replacement of surface hydroxyls of TiO_2 by more electronegative fluorine [15]. Takita et al. [21] suggested that the formation of CFC-13 is due to the reaction between the surface F^- species and CFC-12. More directly, Bickle et al. [18] reported that the formation of CFC-114 in the CFC-113 decomposition reaction is due to the reactions: Zr–OH + HF → Zr–F + H_2O and Zr–F + CFC-113 ($C_2F_3Cl_3$) → CFC-114 ($C_2F_4Cl_2$) + Zr–Cl. Similar F/Cl exchange mechanism for fluorination of CFC-113 was proposed by Brunet et al. [43].

Combined with their conclusions, the formation of CFC-13 on metal oxides can be naturally generalized as follows: M–OH + HF → M–F + H_2O; M–F + CFC-12 (CCl_2F_2) → CFC-13 ($CClF_3$) + M–Cl. So it seems that surface

Table 2
Effect of calcination temperature on the selectivity to CFC-13, catalyst: 0.4 g

Catalyst	Selectivity to CFC-13 (%)					
	Calcination temperature (°C)					
	400	500	550	600	700	800
WTi0.2–*m*	0.51	0.29	0.25	0.21	0.11	–
WSn0.2–*m*	–	0.59	–	0.42	0.31	0.27
WFe0.2–*m*	1.32	0.45	–	0.28	0.21	0.20

Table 3
The surface areas of WTin–500

	WO_3 content (g/g TiO_2)						
WTin–500	0	0.1	0.2	0.3	0.4	0.5	0.6
Surface area (m^2/g)	10.6	75.4	93.0	115.6	119.1	102.8	99.9

M–OH plays an important role on the formation of CFC-13. Unmodified metal oxides were relatively easy to be fluorinated by HF produced during the reaction because all the surface M–OH were exposed to HF without protection, thus producing more CFC-13. As for WO_3-modified metal oxides, amorphous tungsten oxide species highly dispersed on the surface [37,38] gave the surface M–OH less opportunity to meet with and be fluorinated by HF. As a result, very little CFC-13 was produced on WO_3-modified metal oxides. This so-called ''covering the surface–inhibiting the fluorination'' effect was also mentioned by Ng et al. [12].

Furthermore, from Tables 1 and 2, it's interesting to note that the selectivity to CFC-13 at T_{100} decreased with the WO_3 loading and it also decreased with the calcination temperature.

As shown in Table 3, the SSA of WO_3-supported TiO_2 ranged slightly between 75.4 and 115.6, while the WO_3 content increased multiply, so that the surface coverage of WO_3 is assumed to increase with the WO_3 content. LRS shown in Fig. 7 also confirmed this assumption: the position of the Raman peak at $\sim 980\ cm^{-1}$ increased monotonely from 971 to 982 cm^{-1} as the WO_3 content was raised up to 0.6 g/g TiO_2, implying the surface coverage of WO_3 increased with the WO_3 content [37,38]. As the surface coverage increased, HF had less and less opportunity to bump and fluorinate M–OH, then the CFC-13 yield decreased with the WO_3 content.

As for the reason why the CFC-13 yield decreased with the calcination temperature, the SSA of WTi catalysts decreased obviously with the calcination temperatures. They were 115.9, 93.0, 80.9, 54.2 and 37.6 m^2/g, respectively, while the WO_3 loading was 0.2 g/g metal oxides constantly, so that the surface coverage of WO_3 is also assumed to increase with the calcination temperature. In addition, the position of the Raman peak at $\sim 980\ cm^{-1}$ increased monotonely from 974 to 990 cm^{-1} as the calcination temperature was raised up to 700°C, also implying that the surface coverage of the supported tungsten oxide species increased with the calcination temperature [37,38]. As the surface coverage increased, the amorphous tungsten oxide species protected the TiO_2 surface more and more perfectly so that HF had less and less opportunity to bump and fluorinate M–OH; then the selectivity to CFC-13 decreased concurrently. In all, the selectivity to CFC-13 decreased with the surface coverage.

3.4. Catalyst life

The catalyst life is an important factor for practical use. In our results, the catalytic activity of WO_3/TiO_2, WO_3/SnO_2 and WO_3/Fe_2O_3 catalysts all remained steady for 120 h on stream (Fig. 8).

The XRD patterns of WTi0.4–500, WSn0.2–600 and WFe0.3–500 before and after the reaction for 120 h are all shown in Fig. 9. As can be seen, all the peaks of WTi, WSn and WFe samples can be assigned to anatase TiO_2, anatase SnO_2 and α-Fe_2O_3, respectively. No obvious difference was found for the XRD patterns of

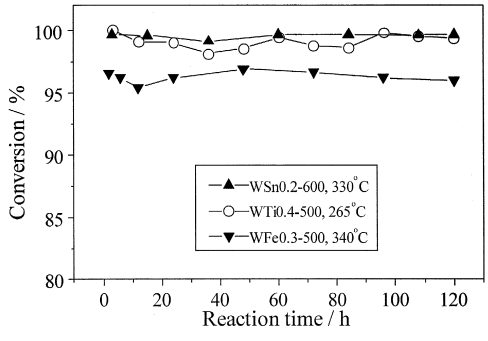

Fig. 8. Conversion of CFC-12 over WTi0.4–500, WSn0.2–600 and WFe0.3–500 during 120 h on stream, catalyst: 0.4 g.

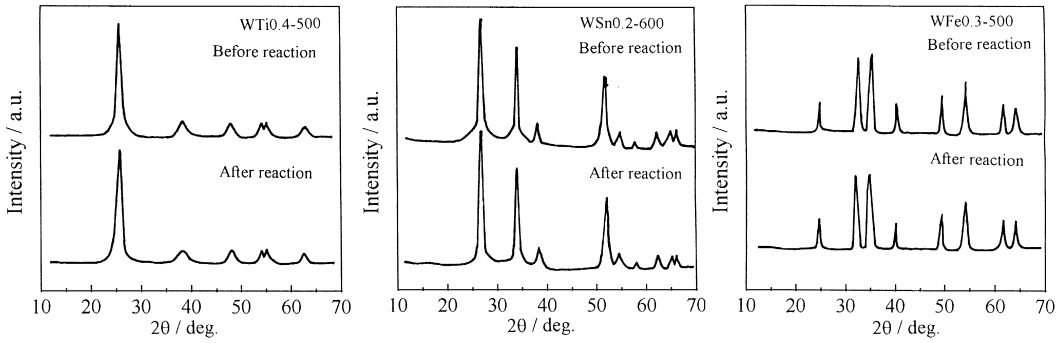

Fig. 9. XRD patterns of WTi0.4–500, WSn0.2–600 and WFe0.3–500 catalysts before and after the CFC-12 decomposition for 120 h.

the fresh and used catalysts, and no diffraction peaks derived from metal fluorides were detected, either. Furthermore, no carbon deposit was detected by elementary analysis. The specific surface area, pore volume and the most probable pore diameter of these samples listed in Table 4 only changed slightly after the stability test and no significant change in pore size distribution was observed either.

Our results may be surprising because it was believed by many researches that all of the metal oxides would be deactivated easily in the reaction since some metal oxides such as Al_2O_3, SiO_2, Al_2O_3–SiO_2 and SiO_2–TiO_2 were very easy to be corroded by HF. However, the stability data given in Table 5 indicate that the stability behavior of neat TiO_2, SnO_2, Fe_2O_2 and Al_2O_2, SiO_2 were quite different. Al_2O_3 and SiO_2 were deactivated for several hours on stream, while TiO_2, SnO_2, and Fe_2O_3 were stable during the reaction for 120 h. Thus it may be concluded that TiO_2, SnO_2 and Fe_2O_2 are good supports in designing CFC decomposition catalysts, although further modifications are required to improve the acidity (thus activity). In fact, Mizuno [44] reported that it's useful to use anatase TiO_2 as a support or part of a support for the decomposition of CFCs. Tajima [45] found that the CFC-113 conversion on the mechanical mixture of W/ZrO_2–TiO_2 and Pd/ZrO_2–TiO_2 was maintained for 150 h. Bickle et al. [18] reported that the CFC-113 conversion on Pt/ZrO_2 decreased from 99.5% to 98% for 60 h on stream. Thus, though some metal oxides were found to be useless in this reaction, others were relatively useful.

Table 4
Surface area, pore volume and the most probable pore diameter of WTi0.4–500, WSn0.2–600 and WFe0.3–500 before and after 120 h on stream

Catalyst	S_{BET} (m^2/g)	V (cm^3/g)	D[a] (nm)
WTi0.4–500			
Fresh	119.1	0.130	3.79
Used	103.2	0.117	3.78
WSn0.2–600			
Fresh	30.2	0.054	3.46, 14.48
Used	32.4	0.057	3.49, 14.66
WFe0.3–500			
Fresh	83.2	0.158	6.13
Used	73.5	0.150	6.09

[a] Most probable pore diameter.

In addition, the role of water vapor in this reaction cannot be neglected. A contrast experiment was well carried out by Karmaker et al. [15]. They observed that without the supply of water vapor, TiO_2 was irreversibly fluorinated and the CFC-12 conversion on TiO_2 dropped drastically from 98% to 43% for 48 h on stream, but it's of interest to note that the decomposition activity decreased only about 2% for 4 days in the presence of water vapor. Li et al. [46] found that the existence of water vapor suppresses the transformation of fluorides, progresses the formation of CO_2 and prolongs the catalyst life. Takita et al. [19] concluded that treating catalysts with both oxygen and water

Table 5
Conversion of CFC-12 on pure M_xO_y (M = Ti, Sn, Fe, Al, Si) at fixed temperatures as a function of reaction time on stream, catalyst: 0.4 g

Reaction time on stream (h)	CFC-12 conversion (%)				
	TiO_2 (340°C)	SnO_2 (475°C)	Fe_2O_3 (475°C)	Al_2O_3 (365°C)	SiO_2 (495°C)
1	98.4	98.8	99.0	97.5	99.0
3	98.8	98.2	99.2	78.7	92.3
5	98.4	98.3	99.1	73.0	49.8
8	98.8	99.0	99.2	68.2	26.4
24	98.6	100	97.3	68.0	11.9
48	98.1	100	97.5	–	–
72	98.7	100	98.1	–	–
96	97.7	100	98.9	–	–
120	97.7	100	97.8	–	–

vapor promotes the removal of fluoride ions in sub-face layers of the catalysts, which is efficient for the recovery of the activity. That is, the reaction $M{-}F + H_2O \rightarrow M{-}OH + HF$ may occur to prevent the further accumulation of surface fluorine [15,18]. Once the surface fluorine is accumulated, the surface turns to be inactive metal fluorides.

In addition, we'd like to propose that though almost all the catalysts will be corroded by pure HF from theoretical calculation, CFCs in this reaction are generally diluted, thus the produced HF is also dilute. This is the difference between theoretical prediction and practical practice. Furthermore, once the dilute HF was formed, ongoing mixed gases carried it away very quickly so that the concentration of HF was not accumulated. This is an advantage of the catalytic decomposition process. In addition, at such low temperature, the deactivation speed is supposed to be much lower than that at high temperature, according to the Arrhenius equation. That is, at low reaction temperature, HF possesses less kinetic energy to bump the catalyst surface as compared with that at high reaction temperature.

4. Conclusions

WO_3-promoted TiO_2, SnO_2 and Fe_2O_3 were effective for the decomposition of CFC-12 in the presence of water vapor as compared with their parent oxides. Acid centers played an important role on the decomposition activity and this enhancement in activity could be attributed to the generation of acid sites by a combination of two oxides.

Calcination temperature and WO_3 loading influenced the acid properties and specific surface simultaneously (thus the decomposition activity). Generally speaking, amount of acid sites and specific surface area shrinked at high calcination temperature, so that a high calcination temperature was not recommended. The decomposition activity reached a maximum at the monolayer coverage of WO_3. The spontaneous dispersion phenomenon can provide a useful way for the design of efficient catalysts.

The selectivity to by-product CFC-13 on WO_3-modified metal oxides was much lower than unmodified metal oxides. Surface fluorine species was believed to catalyze the F/Cl exchange reaction. It was highly dispersed tungsten oxide species that covered the surface, thus inhibiting fluorination and the yield of by-product CFC-13. Furthermore, the higher the WO_3 coverage, the little the CFC-13.

WO_3/TiO_2, WO_3/SnO_2 and WO_3/Fe_2O_3 were not deactivated for 120 h on stream. TiO_2, SnO_2 and Fe_2O_3 were not deactivated, either, so they were believed to be good supports in designing CFC decomposition catalysts, as compared with SiO_2 and Al_2O_3. Water vapor was believed to be essential in maintaining the

activity. Low concentration of HF and low reaction temperature also contributed in prolonging the catalyst life.

Acknowledgements

This work (a sub-project of Molecular Engineering of Functional Systems) was supported by the National Climbing Project of China as sponsored by the Chinese Ministry of Science and Technology.

References

[1] M.J. Molina, F.S. Rowland, Nature 249 (1974) 810.
[2] W. Brune, Nature 379 (1996) 486.
[3] R.F. Service, Science 270 (1995) 381.
[4] F. Gammie, Nature 374 (1995) 108.
[5] S. Okazaki, A. Kurosaki, Chem. Lett. (1989) 1901.
[6] T. Aida, R. Higuchi, H. Niiyama, Chem. Lett. (1990) 2247.
[7] S. Imamura, Shokubai 34 (1992) 464.
[8] S. Imamura, Catal. Today 11 (1992) 547.
[9] Y. Takita, Shokubai 41 (1999) 284.
[10] S. Karmakar, H.L. Greene, J. Catal. 148 (1994) 524.
[11] M. Tajima, M. Niwa, Y. Fujii, Y. Koinuma, R. Aizaun, S. Kushiyama, S. Kobayashi, K. Mizuno, H. Ohuchi, Appl. Catal. B 12 (1997) 263.
[12] C.F. Ng, S. Shan, S.Y. Lai, Appl. Catal. B 16 (1998) 209.
[13] S. Okazaki, European Patent 0 412 456 A2 (1990).
[14] H. Nagata, T. Takakura, S. Tashiro, M. Kishida, K. Mizuno, I. Tamori, K. Wakabayashi, Appl. Catal. B 5 (1994) 23.
[15] S. Karamaker, H.L. Greene, J. Catal. 151 (1995) 394.
[16] S. Imamura, T. Shiomi, S. Ishida, K. Utani, H. Jindai, Ind. Eng. Chem. Res. 29 (1990) 1758.
[17] M. Tajima, M. Niwa, Y. Fujii, Y. Koinuma, R. Aizawa, S. Kushiyama, S. Kobayashi, K. Mizuno, H. Ochuchi, Appl. Catal. B 14 (1997) 97.
[18] G.M. Bickle, T. Suzuki, Y. Mitarai, Appl. Catal. B 4 (1994) 141.
[19] Y. Takita, T. Ishihara, Catal. Surv. Jpn. 2 (1998) 165.
[20] S. Imamura, K. Imakubo, S. Furuyoshi, H. Jindai, Ind. Eng. Chem. Res. 30 (1991) 2355.
[21] Y. Takita, G.L. Li, R. Matsuzaki, H. Wakamatsu, H. Nishiguchi, Y. Moro-oka, T. Ishihara, Chem. Lett. (1997) 17.
[22] H. Wakamatsu, H. Nishigachi, T. Ishihara, Y. Takita, Shokubai 41 (1999) 164.
[23] Y. Takita, M. Ninomiya, R. Matsuzaki, H. Wakamatsu, H. Nishigachi, T. Ishihara, Phys. Chem. Chem. Phys. 1 (1999) 2367.
[24] T. Lei, J.S. Xu, Z. Gao, Mat. Chem. Phys. 60 (1999) 177.
[25] T. Lei, J.S. Xu, Z. Gao, Chem. Lett. 6 (1999) 509.
[26] Y.D. Xia, W.M. Hua, Z. Gao, Appl. Catal. A 185 (1999) 293.
[27] Y.D. Xia, W.M. Hua, Y. Tang, Z. Gao, Chem. Commun. (1999) 1899.
[28] T. Lei, J.S. Xu, W.M. Hua, Y. Tang, Z. Gao, Catal. Lett. 61 (1999) 213.
[29] T. Lei, Y. Tang, J.S. Xu, W.M. Hua, Z. Gao, Appl. Catal. A 192 (2000) 181.
[30] M. Hino, K. Arata, Bull. Chem. Soc. Jpn. 67 (1994) 1472.
[31] Q.Z. Li, Q.X. Cao, W.B. Zhong, A.L. Zhong, J.F. Hu, Chin. J. Catal. 4 (1981) 288.
[32] H.M. Zhang, H. Singu, K. Saeki, S. Morikawa, Shokubai 41 (1999) 111.
[33] G.L. Li, H. Nishiguchi, T. Ishihara, Y. Moro-oka, Y. Takita, Appl. Catal. B 16 (1998) 309.
[34] S. Okazaki, Shokubai 10 (1968) 242.
[35] K. Tanabe, T. Sumiyoshi, K. Shibata, T. Kiyoura, J. Kitagawa, Bull. Chem. Soc. Jpn. 47 (1974) 1064.
[36] T. Yamaguchi, Y. Tanaka, K. Tanabe, J. Catal. 65 (1980) 442.
[37] S.S. Chan, I.E. Wachs, L.L. Murell, N.C. Dispenziere, J. Catal. 92 (1985) 1.
[38] S.S. Chan, I.E. Wachs, L.L. Murrell, L. Wang, W.K. Hall, J. Phys. Chem. 88 (1984) 5831.
[39] B.Y. Zhao, Z.J. Kang, C. Li, Y.C. Xie, Y.Q. Tang, Chin. J. Catal. 6 (1985) 219.
[40] B.Y. Zhao, X.P. Xu, H.R. Ma, D.H. Sun, J.M. Gao, Catt. Lett. 45 (1997) 237.
[41] Y.C. Xie, Y.Q. Tang, Adv. Catal. 37 (1990) 1.
[42] X. Fu, W.A. Zeltner, Q. Yang, M.A. Anderson, J. Catal. 168 (1997) 482.
[43] S. Burnet, B. Requieme, E. Colnay, J. Barrault, M. Blanchard, Appl. Catal. B 5 (1995) 305.
[44] K. Mizuno, Y. Hinuma, Japanese Patent Application 3-47516 (1991).
[45] M. Tajima, M. Niwa, Y. Fujii, Y. Koinuma, R. Aizawa, S. Kushiyama, S. Kobayashi, K. Mizuno, H. Ohuchi, Appl. Catal. B 14 (1997) 97.
[46] G.L. Li, T. Ishihara, Y. Moro-oka, Y. Takita, Appl. Catal. B 9 (1996) 239.